

Development of Empirical Models for Estate-Level Air Temperature Prediction in Singapore

Steve Kardinal Jusuf Wong Nyuk Hien

National University of Singapore, Singapore

Corresponding author email: stevekj@nus.edu.sg

ABSTRACT

The urban heat island (UHI) phenomenon has become a common problem in many major cities worldwide, including Singapore. As a small island state, it is very important for Singapore to carefully plan its urban development. However, urban planners have no assessment tool with which to evaluate the impact of their planning on the environment, especially the impact on air temperature due to changes in land use. This paper discusses the development of empirical models for air temperature prediction to evaluate the impact of estate development, by means of the Geographical Information System (GIS).

Empirical models of minimum (T_{\min}), average (T_{avg}), and maximum (T_{\max}) air temperature for Singapore estate have been developed and validated, based on long-term field measurements made between September 2005 and March 2008. The independent variables used in these models are *daily minimum* ($T_{\min-r}$), *average* ($T_{\text{avg-r}}$), and *maximum* ($T_{\max-r}$) temperature at reference point, *average of daily solar radiation* (SOLAR), *percentage of pavement area over radius 50 m surface area* (PAVE), *average height-to-building area ratio* (HBDG), *total wall surface area* (WALL), *green plot ratio* (GnPR), *sky view factor* (SVF), and *average surface albedo* (ALB).

Sensitivity analyses were carried out to observe the dependence of the air temperature due to the variations of each variable. An ideal type of urban canyon was used to simplify the variation of building, pavement, and greenery distributions. The sensitivity analyses were carried out by varying some of the following important parameters: the green plot ratio, or greenery density (GnPR), which can affect the SVF; the building height, which affects the SVF, WALL, and HBDG values; and canyon width, which affects the SVF, PAVE, and HBDG values.

The Screening Tool for Estate Environment Evaluation (STEVE) was developed with the intention of bridging research findings, especially those of air temperature prediction models and of urban planners.

Introduction

Urban development is imperative for economic growth and national development. The over-development of cities, as compared with the rate of development in neighboring towns and villages, attracts more inhabitants to cities, leading to an urgent need to further develop those cities. According to Laski and Schellekens (2007), in 2008, more than half of the world's population lived in urban areas, and the number was expected to reach 5 billion people by 2030.

The problem of urbanization is not limited to Singapore. Urbanization in this city-state extends beyond its borders to neighboring countries and even more broadly to other countries of Southeast Asia. Known as the most politically stable and

safest country in Asia, Singapore attracts a large pool of foreign talent and traders from all over the world. Furthermore, the government has a plan to increase the population from the current 4.5 million to 6.5 million within 40 to 50 years (AP, 2007). New urban development can be expected to accommodate the social and economical needs of the growing population. With its current inhabitants and limited land area of 707.1 km², Singapore has already become the third most densely populated independent country in the world, after Macau (China) and Monaco (see Wikipedia, 2012). Without careful urban planning that incorporates environmental sustainability, the urban climate may suffer adverse consequences, such as the development of an urban heat island (UHI), thermal discomfort, and pollution. The details of Singapore's urban planning concept

were described in the 2001 Concept Plan. However, environmental impact assessment is not a mandatory requirement of Singapore's urban development. Furthermore, urban planners have no assessment tools and methods with which to evaluate the impact of their planning on the environment.

Closely related to urbanization, UHI has become a common problem in many major cities worldwide (Oke 1971; Padmanabhamurty 1990/91; Sani 1990/91; Swaid and Hoffman 1990; Eliasson 1996; Giridharan et al. 2007) as well as in Singapore (Wong and Chen 2009). This phenomenon is mainly due to the loss of greenery area for the purpose of urban development.

This paper discusses the development of empirical models for air temperature prediction to evaluate the impact of estate development, by means of the Geographical Information System (GIS).

Background studies (Wong et al. 2007; Jusuf et al. 2007; Wong and Jusuf in submission) have been conducted to investigate the existence of temperature patterns in relation to urban morphology conditions, which is important for the development of air temperature prediction models. This research concluded the existence of a temperature pattern that is closely related to urban land use. It was found that during daytime, industrial areas exhibit a higher surface temperature than do commercial and business areas, and that park areas have the lowest surface temperature. However, at night, commercial and business areas exhibit a higher ambient temperature than do industrial and airport areas. The industrial areas are characterized by low building height, large pavement areas, less vegetation, and light roof structures that provide little shading and have extensive use of heat absorbing building materials. As a result, this pattern has high daytime temperatures. On the other hand, it has cool nighttime temperatures because heat stored during the daytime is easily released into the sky at night, with little obstruction from surrounding buildings. This proposed temperature pattern indicates a relationship between the surrounding greenery, buildings, and pavement.

Hence, we propose the following hypothesis for urban air temperature: The air temperature of a point at a certain height is

the function of the local climate characteristics, which vary according to the surrounding urban morphology characteristics (i.e., buildings, pavement, and greenery) at a *certain radius*.

Methodology

Air temperature prediction models

The field-measurement data for the model's development were collected between September 2005 and March 2008. Meanwhile, field-measurement data collected between April and June 2008 were used for model validation. Table 1 shows the overall period of measurements in National University of Singapore (NUS) and One-North.

HOBO data loggers, together with solar covers, were used in the measurements. They were attached to the lampposts in various locations in NUS and One-North, and were configured at 10-minute intervals throughout the measurement periods. The air temperature data were obtained by sampling at a height of 1.8 m for each of the locations shown in Figure 1. The sensors were factory calibrated.

As a reference point, meteorological data were gathered from a nearby station, which was maintained by NUS (Department of Geography 2008). The data analysis focused on fairly clear, calm (wind speed < 3m/s), hot weather conditions, selected by analyzing the solar radiation, wind speed, and air temperature data of the reference point.

Daily minimum (T_{min}), average (T_{avg}), and maximum (T_{max}) temperatures for each point of measurement were calculated as dependent variables of the air temperature prediction models. The independent variables of the models were categorized as follows:

1. Climate predictors: *daily minimum* (T_{min-r}), *average* (T_{avg-r}), and *maximum* (T_{max-r}) temperature at the reference point; *average of daily solar radiation* (SOLAR). For the SOLAR predictor, the average of the daily solar radiation total (SOLAR_{total}) was used in T_{avg} models, while the average of the solar radiation maximum of the day (SOLAR_{max}) was used in the T_{max} model. The SOLAR predictor is not applicable for the T_{min} model.

Table 1. Overall periods of measurement in NUS and One-North

ESTATE	TYPE OF MEASUREMENT	PERIOD OF MEASUREMENT
NUS	Estate-wide	10th-24th September 2005
NUS	Estate-wide	26th August-25th September 2006
NUS	Canyon (ENG & PGP)*	17th July-20th October 2007
NUS	Canyon (PGP, SD2 & SD4)*	23rd October 2007-31st March 2008
One-North	Estate-wide	23rd October 2007-31st March 2008
One-North	Canyon (AYER, BIO, ROCH)*	23rd October 2007-31st March 2008
One-North	Canyon (AYER, BIO, ROCH)* for model validation	1st April-30th June 2008

* Engineering (ENG), Price George's Park (PGP), Science Drive 2 (SD2), Science Drive 4 (SD4), Ayer Rajah Industrial Estate (AYER), Biopolis (BIO), and Rochester Park (ROCH)

2. Urban morphology predictors: *percentage of pavement area over R 50 m surface area (PAVE), average height-to-building area ratio (HBDG), total wall surface area (WALL), green plot ratio (GnPR), sky view factor (SVF), and average surface albedo (ALB).*

Wind speed, one of the most common variables, was excluded from the model's development because the model's focus is on calm daytime conditions. For another common variable, altitude, a Kestrel 4200 pocket weather tracker was used to measure the altitude of each measurement point. The measurement results indicate that the altitude difference across

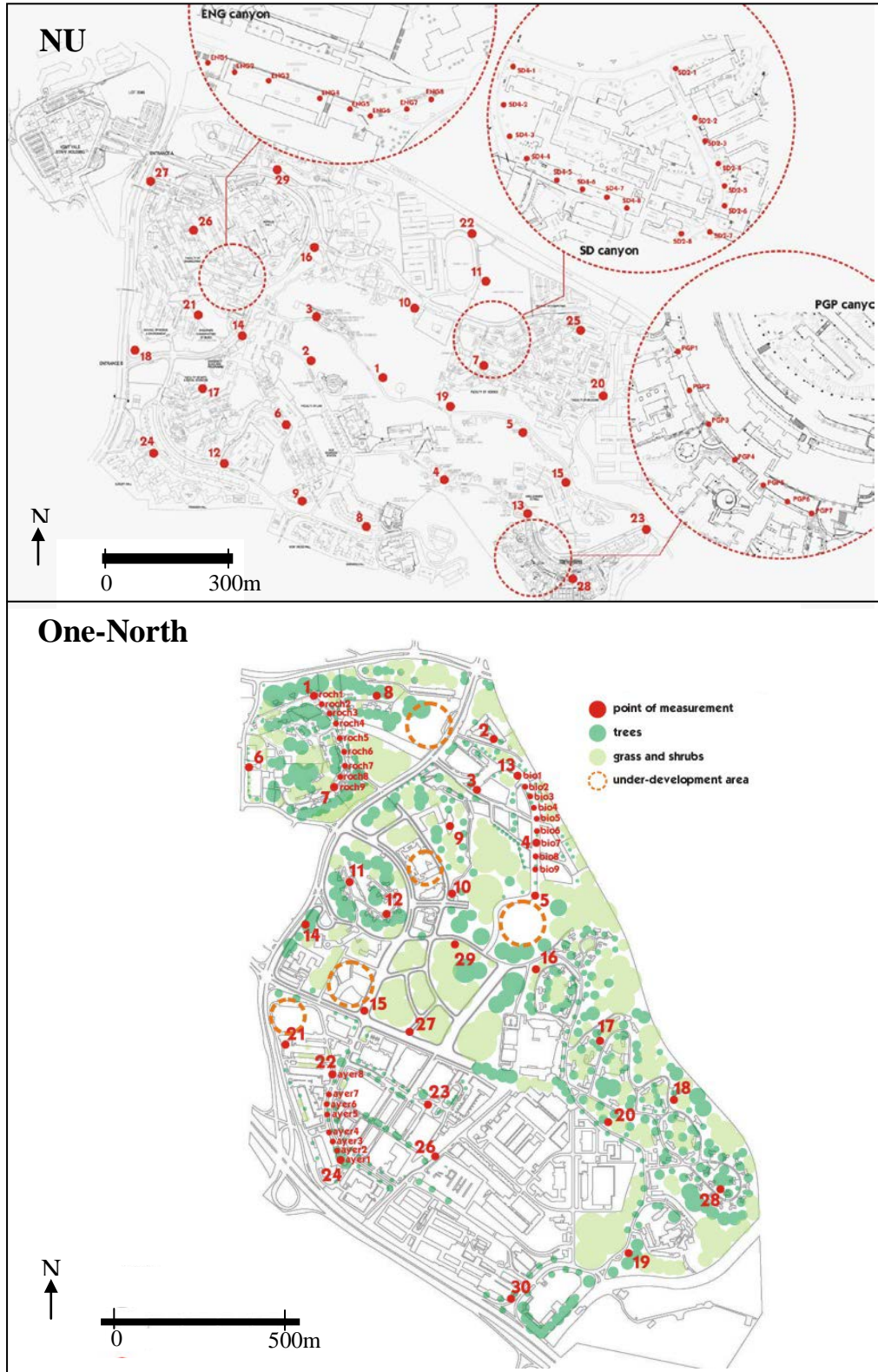


Figure 1. Points of measurements at the NUS (above) and One-North (below) sites

the two estates is only about 56 m, which is considered relatively flat. The highest location is 156 m above sea level at Point 1, NUS estate, and the lowest point is 98 m above sea level at Rochester Park, One-North. The 56 m altitude difference will only influence air temperature under ideal conditions of about 0.36 K, based on an atmospheric lapse rate of $-0.0065^{\circ}\text{C}/\text{m}$ (ISO 1975). This means that altitude has very little influence on air temperature conditions. Hence, altitude was excluded from the model's development.

In collecting the urban morphology predictors, master plan drawings of NUS and One-North were obtained from the relevant agencies and were entered into GIS to quantify the PAVE and WALL areas. Field surveys had been done to verify and update the drawings. Besides the PAVE areas, the building (BDG) and greenery (GREEN) areas were also quantified. BDG was calculated based on a 2-D footprint area, while PAVE and GREEN were calculated in 3-D areas, following the contour of the land surfaces. BDG results were then used to calculate the HBDG variable, while GREEN was used to calculate the GnPR variable. HBDG represents the thermal mass of the environment within the radius of the influence area by calculating the ratio of average building height over the total floor area (Knowles 1977; Giridharan et al. 2008). The WALL variable indicates the building density in the area.

The ALB values were taken by field measurements. Two silicon pyranometers (i.e., one directed to the sky and one directed to the wall) were used together with a data logger, simultaneously mounted on a lamppost, and recorded the solar

radiation for a few days, weather conditions permitting. Then the pyranometers were moved and redirected to different locations to record the albedo of the surrounding environment.

The SVF of each measurement point was measured by means of a Nikon digital camera and fisheye lens. The images were processed in black and white, so the sky was white and the buildings and trees black. Then the images were put into RayMan 1.2 software to calculate the SVF (Matzarakis 2000).

Before the models were developed, the radius of the influence area was determined. Giridharan et al. (2007) used a 15 m to 17.5 m radius as the influence area to study the effect of greenery and found that a 15 m to 17.5 m radius was not able to explain the significant impact to the air temperature. Meanwhile, Kruger (2007) studied three different influence area radii of 56 m, 125 m, and 565m and found that a radius of 56 m had a significant effect on the model's correlation coefficient.

In the preliminary study, four different radii were selected as the most significant for influence areas: 25 m, 50 m, 75 m, and 100 m (Figure 2). The BDG and PAVE areas were correlated with T_{\min} , T_{avg} , and T_{\max} to provide an indication of the radius of the influence area. Table 2 shows that 50 m and 75 m were the top two radii in terms of high F and R^2 values, although the 75 m radius seems to have had the highest F and R^2 . Further selection was done by including all the aforementioned variables and the 50 m radius was found to have a more significant influence area than do the other radii. Consequently, this chapter will analyze and discuss the air temperature prediction models based on a 50 m radius. This result agrees with the Kruger analysis (2007).

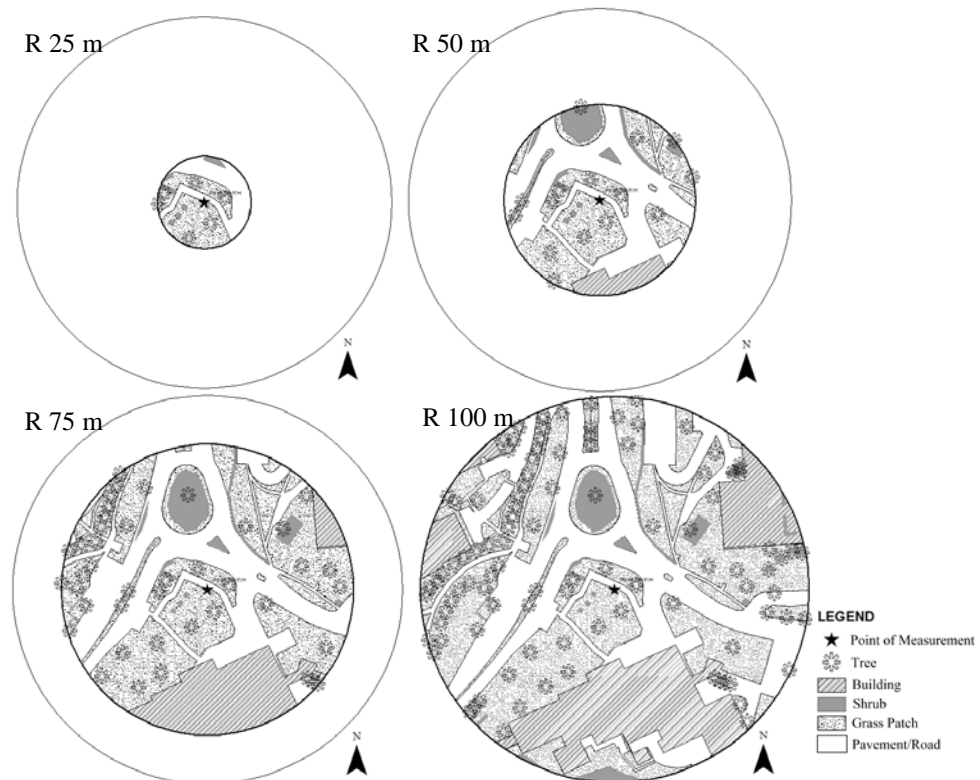


Figure 2. Sample of NUS measurement point in influence area radius of 25 m, 50 m, 75 m, and 100 m

Table 2. Preliminary study of radius of influence area

RADIUS (m)	T_{min}			T_{avg}			T_{max}		
	R^2	F	Significance ($p < 0.05$)	R^2	F	Significance ($p < 0.05$)	R^2	F	Significance ($p < 0.05$)
25	0.28	21.79	YES	0.22	15.13	YES	0.05	3.09	NO
50	0.32	25.84	YES	0.26	19.43	YES	0.10	5.76	YES
75	0.34	28.27	YES	0.29	22.51	YES	0.10	5.96	YES
100	0.31	24.62	YES	0.25	18.64	YES	0.08	4.83	YES

Sensitivity Analysis

The sensitivity analyses were carried out to analyze the dependence of the air temperature on each variable. An ideal type of urban canyon (see Figure 3a) was used to simplify the variation of buildings, pavement, and greenery distributions. Table 3 shows the climatic predictor values at the weather station that were used in this sensitivity analysis, based on the conditions on November 3, 2007, and Table 4 shows the variables modified according to different temperature models for the sensitivity analyses.

The analyses were done by varying some of the following important parameters: the green plot ratio (GnPR), which can affect the SVF; the building height, which affects the SVF, WALL, and HBDG values; and canyon width (Figure 3b), which affects the SVF, PAVE, AND HBDG values.

In relation to the above building-layout models, given a fixed surface area of 50 m radius, the change of GnPR depends

on the species (Leaf Area Index, or LAI) and numbers of the plants, regardless the height of the plants (shrubs or trees). In these sensitivity analyses and model application studies, only the increase of GnPR due to trees was considered, whereby trees can reduce the SVF value. Therefore, it is necessary to derive an estimate of how much reduction in the SVF value is due to the increase of 1 GnPR.

To derive the estimated SVF reduction value, 46 of the 110 measurement points were statistically analyzed (see Table 5). Of these 46 measurement points, mature trees had the predominant influence on the GnPR, which in turn, affected the SVF values. From the regression result, eqn. 1, it can be estimated that the SVF value is reduced by about 0.2 for every GnPR increase of 1.

$$SVF = 0.962 - 0.219 \text{ GnPR} \tag{1}$$

$$R^2 = 0.44 \text{ and } F = 35.17(p < 0.01)$$

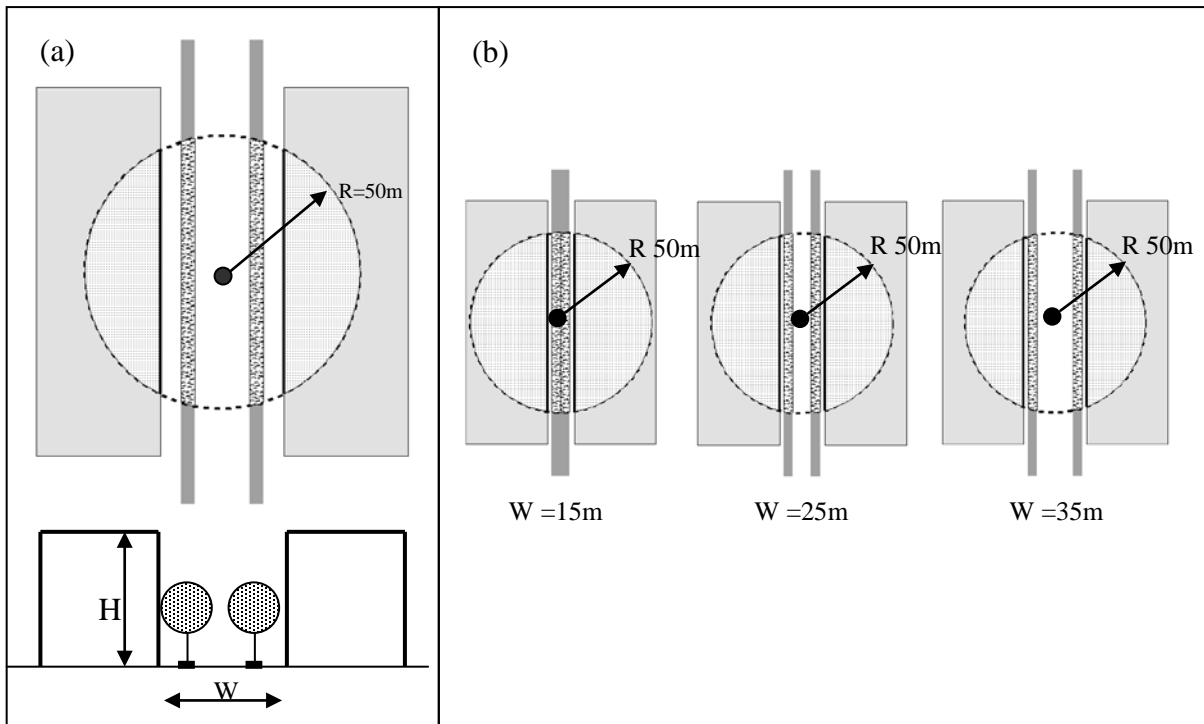


Figure 3. (a) Building layout model for sensitivity analysis and (b) building layout model 3 on change of canyon width

Table 3. Input on climate predictors, based on data at weather station

Date	3 November 2007
Min. Temp. at reference point (Ref Tmin)	26.0 °C
Avg. Temp. at reference point (Ref Tavg)	27.7 °C
Max. Temp. at reference point (Ref Tmax)	30.6 °C
Total solar radiation (SOLAR _{total})	3689.04 W/m ²
Max. solar radiation (SOLAR _{max})	707 W/m ²

Table 4. Model scenarios for the sensitivity analyses

		Model 1	Model 2	Model 3
Variables to be modified		GnPR	No of storey, GnPR	Canyon Width, GnPR
Parameters	No of storeys (@ 4m)	4	1-60 (Even no)	4
	Canyon width	45m	45m	15m, 25m, 35m, 45m
	Greenery strips width	5m	5m	5m
	GnPR	0, 1, 2, 3, 4, 5, 6, 7, 8	0, 1, 2, 3, 4, 5, 6	0, 1, 2, 3, 4, 5, 6

Table 5. The selected 46 measurement points

ESTATE	POINT NAME	ESTATE	POINT NAME	ESTATE	POINT NAME	ESTATE	POINT NAME
NUS	POINT 1	NUS	POINT 17	One-North	POINT 10	One-North	POINT 28
NUS	POINT 2	NUS	POINT 18	One-North	POINT 11	One-North	POINT 30
NUS	POINT 3	NUS	POINT 21	One-North	POINT 12	One-North	BIO 1
NUS	POINT 5	NUS	POINT 22	One-North	POINT 13	One-North	ROCH 2
NUS	POINT 6	NUS	POINT 24	One-North	POINT 14	One-North	ROCH 3
NUS	POINT 8	NUS	POINT 25	One-North	POINT 15	One-North	ROCH 4
NUS	POINT 9	NUS	POINT 30	One-North	POINT 16	One-North	ROCH 5
NUS	POINT 10	One-North	POINT 1	One-North	POINT 17	One-North	ROCH 6
NUS	POINT 11	One-North	POINT 5	One-North	POINT 18	One-North	ROCH 7
NUS	POINT 12	One-North	POINT 7	One-North	POINT 19	One-North	ROCH 8
NUS	POINT 15	One-North	POINT 8	One-North	POINT 20	One-North	ROCH 9
NUS	POINT 16	One-North	POINT 9	One-North	POINT 27		

Results and Discussions

Air temperature prediction model

Model development. In the first stage of model development, a trend analysis was done to identify and discuss the behavior of the respective models' variables, by examining the variables' regression coefficient values and their correlations with the dependent variable (Pearson correlation). Not all the independent variables were significant; however, it is important to analyze how these variables behave in determining the air temperature. Table 6 shows the regression results for T_{min} , T_{avg} , and T_{max} models. The correlation coefficients for the T_{min} and T_{avg} models are high, at 0.86 and 0.92, respectively, while the correlation coefficient is fair, at 0.54, for the T_{max} model.

The SOLAR, PAVE, HBDG, and WALL variables in all the models are in line with the general theory of factors that influence air temperature. Both values (i.e., negative and positive) are the same in the regression and Pearson correlation results.

In general, extensive use of concrete and other heat-absorbing surfaces (PAVE) increases urban air temperature by decreasing the surface moisture available for

evapotranspiration. Furthermore, more solar radiation is absorbed and reradiated into heat because dry surfaces have a low albedo (ALB) value (Santamouris 2001).

The HBDG and WALL of each point are in line with the general theory. They have negative and positive values, respectively, in both the regression coefficient and Pearson correlation results. The higher the thermal mass of the environment, the lower the temperature because the heat released into the surrounding environment is reduced. Meanwhile, a large WALL leads to a higher air temperature because the WALL reflects shortwave and longwave solar radiation to the environment.

Greenery is one of the important factors in Singapore's urban development. It shapes the pleasant urban environment. The multiple regression models verify that greenery, noted as GnPR, has a positive impact on the environment. It reduces the air temperature, as shown in negative values in both the regression coefficient and Pearson correlation in the T_{min} and T_{avg} models. However, in the T_{max} model, GnPR has positive and negative values in the regression coefficient and Pearson correlation results, respectively. It is believed that the existence of anthropogenic heat further increases air temperature, and thus

Table 6. Regression results of air temperature prediction models

VARIABLES	T _{min}			VARIABLES	T _{avg}			VARIABLES	T _{max}		
	R 50M				R 50M				R 50M		
	B	Sig.	Pearson Correlation		B	Sig.	Pearson Correlation		B	Sig.	Pearson Correlation
Constant	3.548			Constant	1.842	0.00		Constant	7.511		
T _{min-r}	0.848	0.00	0.89	T _{avg-r}	0.915	0.00	0.91	T _{max-r}	0.684	0.00	0.50
SOLAR _{total}	NA	NA	NA	SOLAR _{total}	5.782E-05	0.00	0.50	SOLAR _{max}	0.0030	0.00	0.15
PAVE	0.003	0.00	0.27	PAVE	0.007	0.00	0.34	PAVE	0.006	0.00	0.24
GnPR	-0.159	0.00	-0.18	GnPR	-0.037	0.00	-0.23	GnPR	0.009	0.52	-0.28
HBDG	-0.030	0.00	-0.13	HBDG	-0.015	0.00	-0.08	HBDG	-0.016	0.00	-0.03
WALL	1.674E-05	0.00	0.40	WALL	1.539E-05	0.00	0.42	WALL	7.391E-06	0.00	0.19
SVF	0.113	0.07	-0.06	SVF	0.614	0.00	0.07	SVF	1.475	0.00	0.39
ALB	0.911	0.00	-0.09	ALB	0.991	0.00	-0.01	ALB	1.492	0.00	0.23
F	1240.77			F	1994.50			F	211.57		
R ²	0.86			R ²	0.92			R ²	0.54		
Std Error	0.47			Std Error	0.27			Std Error	0.59		

NOTE: Daily minimum (T_{min-r}), average (T_{avg-r}), and maximum (T_{max-r}) temperature at reference point; average of daily solar radiation (SOLAR); percentage of pavement area over a radius of 50 m surface area (PAVE); average height-to-building area ratio (HBDG); total wall surface area (WALL); green plot ratio (GnPR), sky view factor (SVF); and average surface albedo (ALB).

the greenery effect becomes less significant.

The SVF variable has a positive value in all the models, which seems not in line with the general theory that a low SVF leads to high nocturnal air temperature (Oke 1981; Oke et al. 1991; Chapman et al. 2001). A detail study has been done and discussed that investigated the correlation between air temperature and SVF in Singapore (Wong and Jusuf in submission). The study concluded that during daytime, a strong correlation exists between air temperature and SVF. The higher SVF leads to a higher air temperature, which means no obstruction prevents solar radiation from heating up the environment. For nighttime, specifically at around 05.00 to 07.00 hours, a very weak correlation was found between air temperature and SVF, in line with the aforementioned general theory. The findings support the multiple regression model results. In the T_{avg} and T_{max} models, the SVF has both positive values in the regression coefficient and Pearson correlation results. Furthermore, these values are significant in relation to air temperature conditions. In the T_{min} model, however, the SVF has a positive value in the regression coefficient results and a negative value in Pearson correlation results.

In all the models, the ALB variable shows a positive value in the regression coefficient results, which is against the general theory. However, in the T_{min} and T_{avg} models, the correlation values are negative, while it is positive in the T_{max} model. According to Taha et al. (1988), the range of natural environment albedo is narrower than the range of individual building material. The existence of greenery at most of the measurement points also leads to less variation in the ALB variable. Furthermore, anthropogenic heat is believed to have influenced the results because some of the areas had large

pavement areas under construction. During daytime, when maximum air temperature is reached, ground surfaces absorb heat and radiate it over time, rather than reflect it immediately. Consequently, the ALB value behaves against the general theory, but it explains the phenomenon in this research (Giridharan et al. 2008).

The next stage was to develop air temperature prediction models that use only the significant variables (p < 0.05). Variables that had an opposite value for regression coefficient and Pearson correlation analyses have been removed.

Hence, the air temperature prediction models can be written as follows:

$$T_{min} (^{\circ}C) = 4.061 + 0.839 T_{min-r} + 0.004 PAVE - 0.193 GnPR - 0.029 HBDG + 1.339E-06 WALL$$

$$R^2 = 0.86, F = 1707.45 \text{ and Std. Error} = 0.47 (p < 0.01) \quad (2)$$

$$T_{avg} (^{\circ}C) = 2.347 + 0.904 T_{avg-r} + 5.786E-05 SOLAR_{total} + 0.007 PAVE - 0.06 GnPR - 0.015 HBDG + 1.311E-05 WALL + 0.633 SVF$$

$$R^2 = 0.91, F = 2170.49 \text{ and Std. Error} = 0.27 (p < 0.01) \quad (3)$$

$$T_{max} (^{\circ}C) = 7.542 + 0.684 T_{max-r} + 0.003 SOLAR_{max} + 0.005 PAVE - 0.016 HBDG + 6.777E-06 WALL + 1.467 SVF + 1.466 ALB$$

$$R^2 = 0.54, F = 241.92 \text{ and Std. Error} = 0.59 (p < 0.01) \quad (4)$$

NOTE: daily minimum (T_{min-r} - °C), average (T_{avg-r} - °C) and maximum (T_{max-r} - °C) temperature at reference point; average of daily solar radiation (SOLAR - W/m²); percentage of pavement area over radius 50 m surface area (PAVE - %); average height-to-building area ratio (HBDG); total wall surface area (WALL - m²); green plot ratio (GnPR);

sky view factor (SVF); and average surface albedo (ALB).

Models validation The air temperature multiple regression models were developed based on data over a few years. It is necessary to validate the models with another period of measurement data, which in this case was fairly clear and calm day conditions (wind speed < 3 m/s).

Figure 4 shows the validation of minimum air temperature model (T_{min}). It shows that the calculated minimum air temperature matches the measured one. From the box and whisker plot, it can be seen that 50% of the difference between the calculated and measured minimum air temperatures is within acceptable range of -0.3°C to 0.5°C .

The validation of average air temperature models is shown

in the Figure 5. Similar to the minimum air temperature model (T_{min}), the calculated result of average air temperature model (T_{avg}) matches the measured one. It can be seen from the box and whisker plot that 50% of the difference between the measured and calculated average air temperatures is between -0.1°C and 0.4°C .

Lastly, Figure 6 shows the validation for the maximum air temperature multiple regression model (T_{max}). This model has a fair R^2 value of 0.54. From the comparison graph, it can be observed that, at some points, the difference between the measured and calculated results is relatively large, more than 1°C . It is believed that the existence of anthropogenic heat, which is not covered in the model, has influence on the prediction model. On the other hand, as shown in the box and whisker plot,

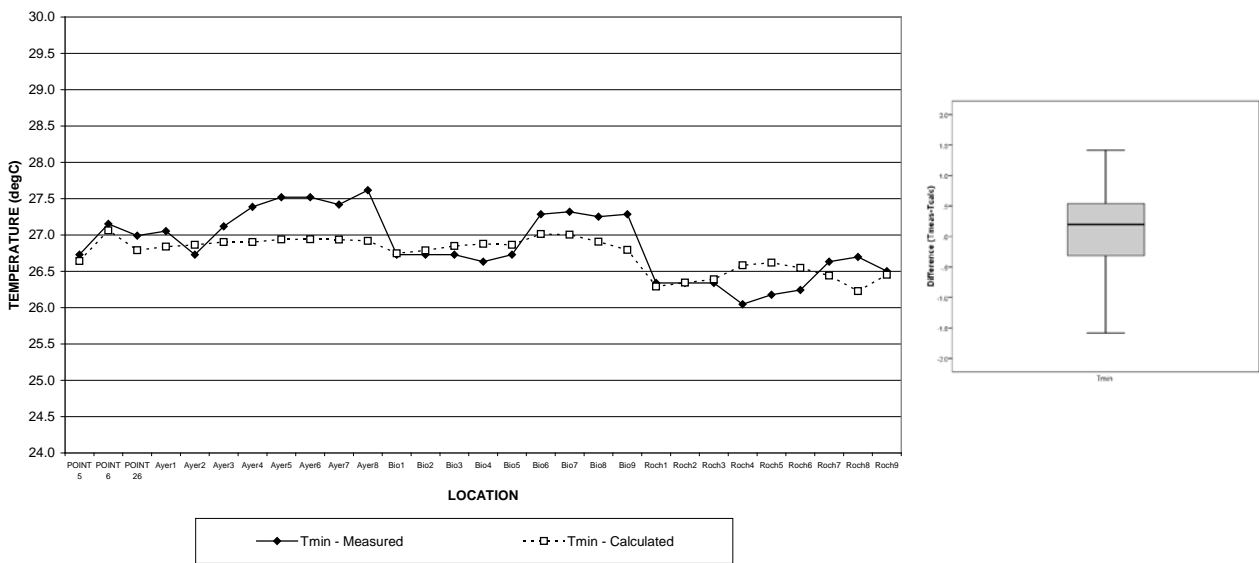


Figure 4. The comparison between measured and calculated minimum air temperature (T_{min}) and the box and whisker plot of the minimum air temperature difference between measured and calculated temperatures

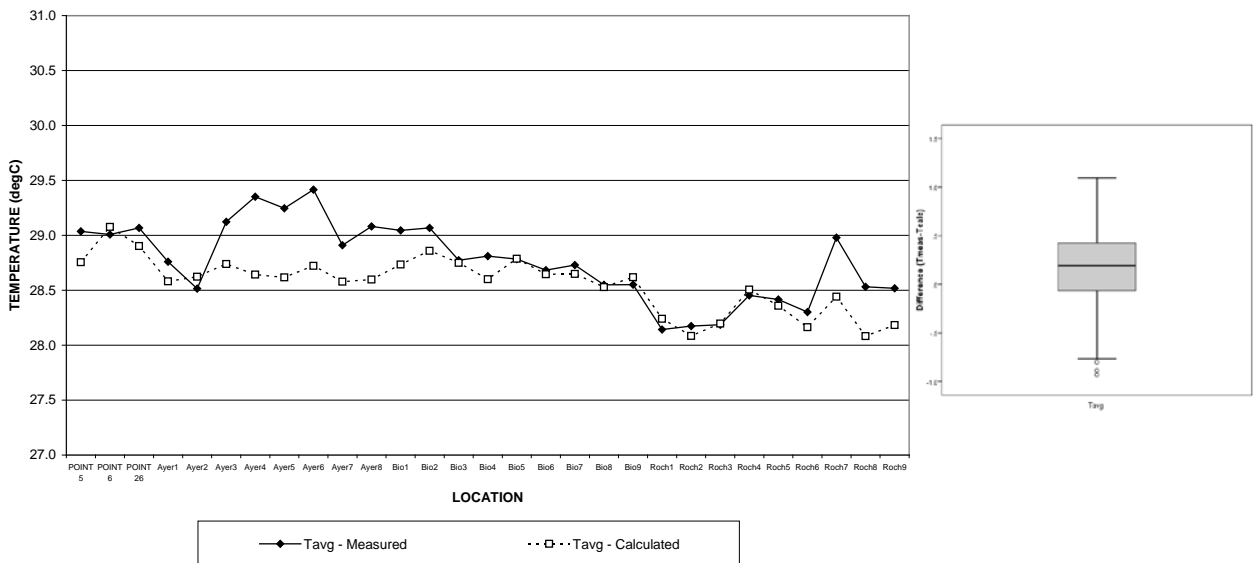


Figure 5. The comparison between measured and calculated average air temperature (T_{avg}) and the box and whisker plot of the average air temperature difference between measured and calculated temperatures

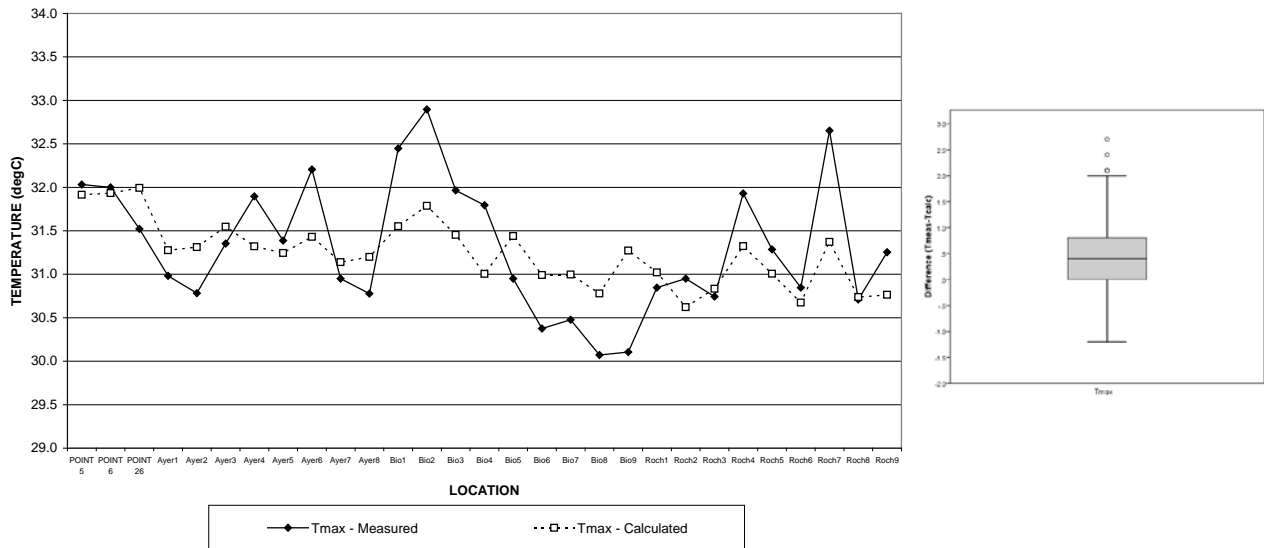


Figure 6. The comparison between measured and calculated maximum air temperature (T_{max}) and the box and whisker plot of the maximum air temperature difference between measured and calculated temperatures

50% of the difference between the calculated and measured maximum air temperatures is between 0°C and 0.8°C . Thus, although the difference is larger than in the minimum and average temperature multiple regression models, this model can still be used.

Sensitivity Analysis

The effect of the SVF reduction due to greenery varies according to the behavior of the predicted T_{min} , T_{avg} , and T_{max} (see Figure 7). The increase of GnPR mainly governs the reduction of minimum air temperature, shown as a straight line. Meanwhile, in the T_{avg} model, both GnPR and SVF influence the average temperature. When no greenery is present on site (GnPR = 0), the SVF is determined mainly by canyon geometry. Greenery provides shading to the environment (and reduces the SVF); thus, it reduces air temperature. The reduction of average temperature is more prominent when GnPR is increased between

0 and 4 due to the combined factors of GnPR and SVF. Once greenery completely covers the openness to the sky, only GnPR reduces the average air temperature, shown as a broken slope line. On the other hand, GnPR has an indirect impact on the maximum air temperature. The increase of greenery density affects the openness to the sky and thus reduces the maximum air temperature through its shading effect. Hence, as seen in Figure 7, when trees have provided complete shading to the canyon, at a GnPR of 4, the increase of GnPR causes no further reduction in maximum air temperature.

The change of building height seems to have relatively unnoticeable change on minimum air temperature, as shown in Figure 8a. The WALL area, together with the environment's thermal mass, increases when buildings get higher. A very small difference between WALL and HBDG contributes to the reduction of minimum air temperature. The minimum air temperature reduction is still mainly influenced by GnPR. The

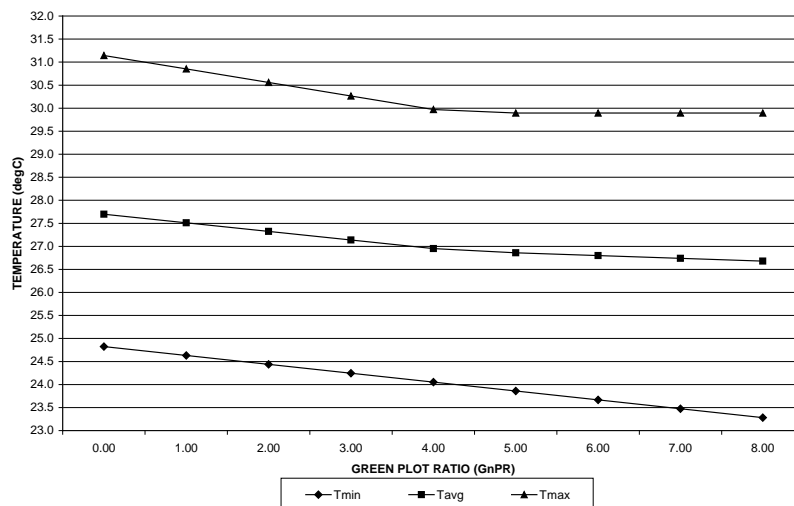


Figure 7. Predicted T_{min} , T_{avg} , and T_{max} for various values of GnPR

influence of building height on the predicted average air temperature is clear (see Figure 8b). As seen in the V profile in the graph (GnPR = 0), the average air temperature is reduced when the HBDG is between 2 and 16. The increase of building height reduces SVF by providing shading. Once the canyon is completely shaded by the surrounding buildings, any further increase of building height, which further increases the WALL areas and the HBDG, will result in an increased average air temperature. When the greenery density is increased, the turning point of the graph (from reduced into increased average air temperature) shifts toward lower building heights, revealing the effect of GnPR in terms of reducing the SVF value.

Similar behavior has been noted for the predicted maximum air temperature (see Figure 8c). However, because GnPR has an indirect relationship with the maximum air temperature through its relation with SVF, the reduction of maximum air temperature stops at GnPR = 5. Once the canyon is completely shaded, either due to buildings or to greenery, the building density becomes the main contributor to the increase of maximum air temperature. The maximum air temperature is expected to remain at the same level when GnPR is 0 and the number of storeys is 30, and starts to increase when the building height is above 60 storeys.

Figure 9 shows the predicted air temperature due to the increase of canyon width. In the T_{min} model, an increase of canyon width increases the PAVE, which also increases the minimum air temperature, shown as an increasing trend when the canyon width is changed progressively from 15 m to 45 m. Meanwhile, in the T_{avg} and T_{max} models, the increase of average

and maximum air temperatures is governed by the increase of PAVE and SVF values (see Figure 9a and 9b). At the same canyon width (i.e., at 15m), in the T_{avg} model, the reduction of air temperature is governed by both GnPR and its impact on the reduction of SVF. When the greenery completely shades the canyon (SVF = 0), only the GnPR reduces the air temperature. On the other hand, at the same canyon width in the T_{max} model, once the SVF is 0, further increases in the GnPR will not lead to any further reduction in maximum air temperature. Figure 9c shows the GnPR value yields at GnPR = 5.

These sensitivity analyses have shown the relationships between some important urban planning variables. It is important for urban planners to find the optimum solutions for greenery, building characteristics, and pavement distributions. Increasing building height will not always have a negative impact (i.e., increase air temperature). To a certain extent, increasing building height provides shading to the environment. On the other hand, widening the canyon width may have an adverse impact during daytime because it increases openness to the sky, which increases incoming solar radiation. In this situation, greenery has an important role in reducing the air temperature, not only through evaporative cooling but also through shading. In these sensitivity analyses, the GnPR was calculated and limited only to the fixed greenery area and the density of trees. However, in the planning process, within the same radius of 50 m, the greenery area can be increased, for example, by using vertical greenery and rooftop greening because the concept GnPR itself is three-dimensional.

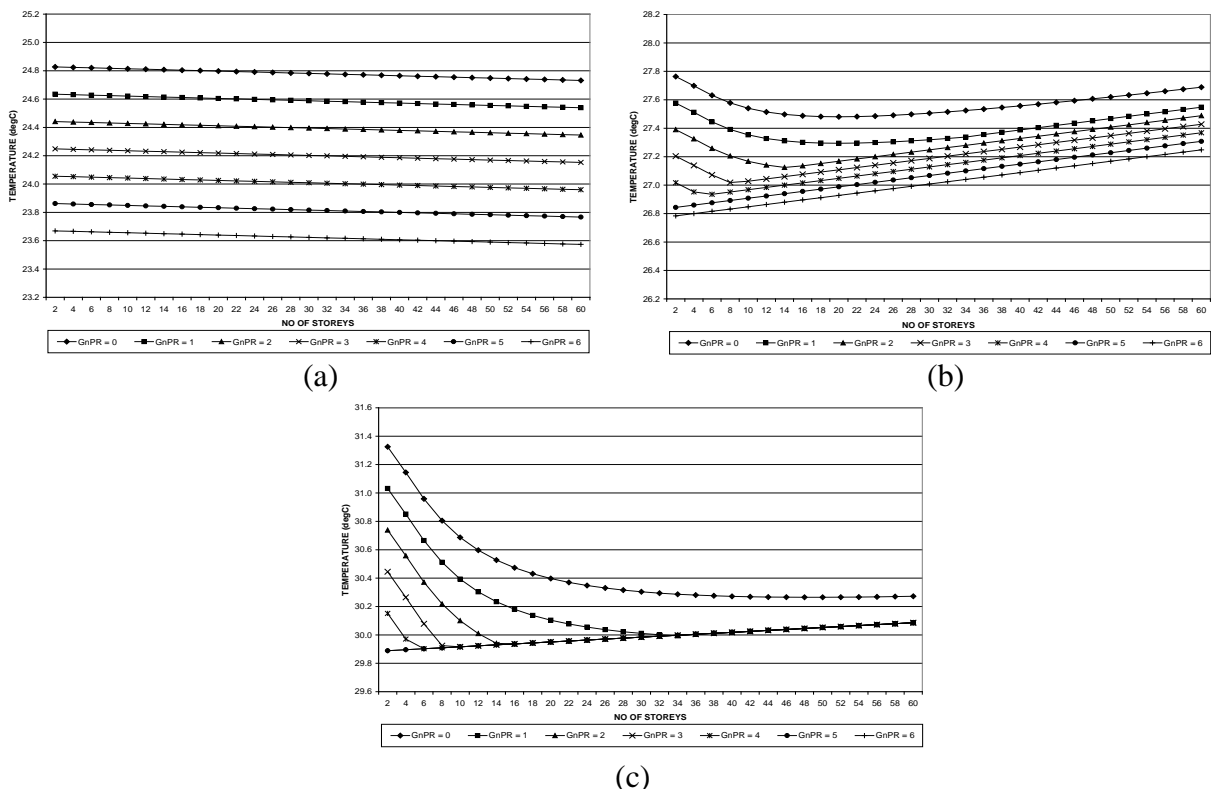


Figure 8. Predicted (a) T_{min} , (b) T_{avg} , and (c) T_{max} for various values for number of storeys and GnPR

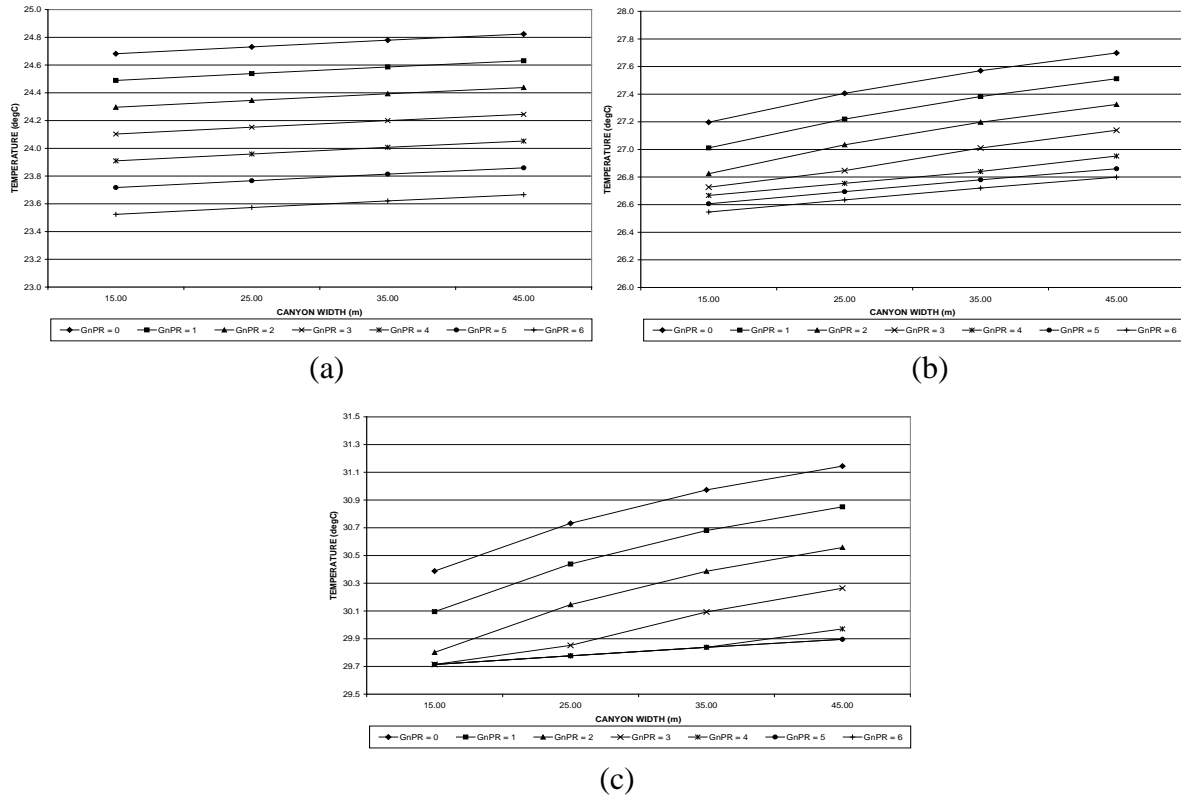


Figure 9. Predicted (a) T_{min} , (b) T_{avg} , and (c) T_{max} for various values of canyon width and GnPR

Screening Tool for Estate Environment Evaluation (STEVE)

STEVE was developed with the intention, as discussed above, of bridging research findings, especially those of air temperature prediction models and urban planners. STEVE is a web-based application that is specific to an estate and calculates the T_{min} , T_{avg} , and T_{max} of a point of interest for the existing condition and future conditions (i.e., proposed master plan) of the estate. The air temperature prediction models discussed above were used in this application. In this version, STEVE was made for One-North estate (see Figure 10) and consisted of three main interfaces: estate's existing condition map, estate's proposed master plan map, and a calculator of air temperature predictions.

Several steps are involved in running STEVE:

1. Select the estate condition: existing site or future development
2. Select a point of location
3. Fill in the various variables listed in the calculator page

Existing Condition or Future Development Interface

Maps of the estate's existing condition and future development are displayed in this interface. The viewing level of the map is set at three levels. In level 1 (Figure 11a), it displays a complete estate map, including the zoning boundaries, which are darkened when the mouse is pointed to

the selected zone. Users are able to zoom into the map at the second view level by clicking either the selected zone or the zoom-in button (Figure 11b). The designated points appear for the users' selection at this viewing level and then users are able to predict air temperature conditions by clicking the selected point. A circle with the radius of 50 m blinks to provide the urban morphology distribution that will influence air temperature at the selected point (Figure 11c).

Calculator Interface

At the left-hand side of the existing or proposed master plan map, the calculator interface appears with preloaded values for different parameters of the selected point (Figure 12). The preloaded values can be changed according to users' need, and the predicted air temperature results will appear with a click on the calculate button.

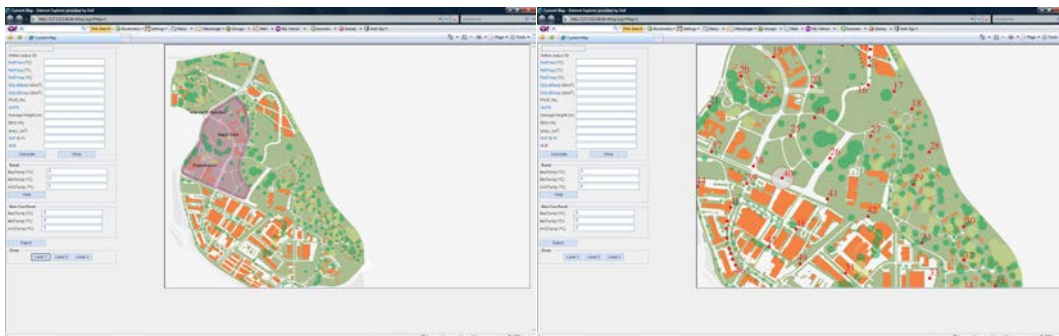
The *climatic predictors*— T_{min-r} , T_{avg-r} , and T_{max-r} (displayed as Ref T_{min} , Ref T_{avg} , and Ref T_{max} , respectively, in the website); $SOLAR_{total}$; and $SOLAR_{max}$ —can be obtained from either a meteorological website or the available recorded data within STEVE by clicking each predictor. The other *urban morphology predictors* (i.e., PAVE, HBDG, WALL, and ALB) are straightforward to obtain. However, the GnPR and SVF predictors are rather complicated. Hence, STEVE also provides GnPR and SVF calculators. A pop-up window will appear for the appropriate calculator when the button for each predictor is clicked.



Figure 10. STEVE’s main menu

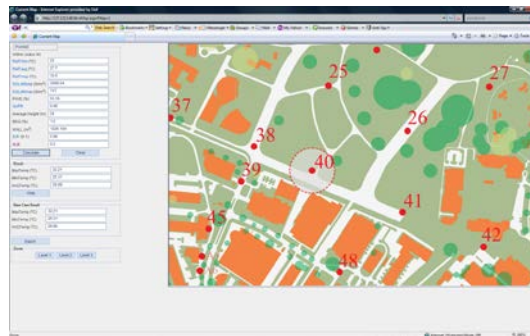
When using the GnPR calculator (Figure 13a), users need to specify up to a maximum of 10 vegetation types, their quantities, and their shade areas. The “Vegetation Type (LAI)” refers to the LAI value of the vegetations, which can be found in the shrubs and trees list. The list has a total of 290 vegetation types. “Shade Area (m²)” refers to the area of vegetation in the plan view. In the case of grass, both

“Vegetation Type (LAI) and “Nos. of vegetation” should be given a value of 1, while “Shade Area (m²)” is the area of the grass itself. “Surface Area (m²)” is the three-dimensional area of a circle with the radius of 50 m when the area is not a flat land surface. Otherwise, it is simply a two-dimensional circle area.



(a)

(b)



(c)

Figure 11. (a) First viewing level of the map, (b) second viewing level of the map, and (c) third viewing level of the map

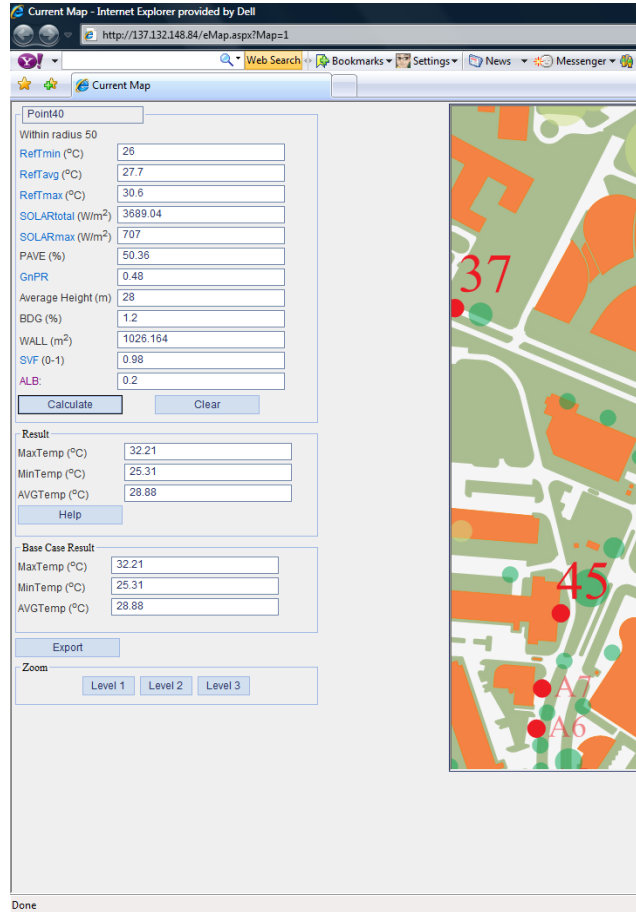


Figure 12. Calculator interface

The SVF calculator (Figure 13b) was developed based on the method by Oke (1981) and the corrected version of the Steyn method (1980) by Barring (1985). Oke estimated the SVF by measuring the height/width ratio of the buildings, with the assumption of an ideal and infinitely long canyon geometry. Meanwhile, in Steyn's method, the SVF obtained from fisheye photographs is considered the real SVF value, as opposed to the Oke method, which was found to underestimate the real SVF value. Barring further corrected the Steyn's method by regressing it with the SVF by Oke's method, as shown in eqn. 8.

The corresponding formulas for the SVF calculator are written as follows:

$$\theta = \tan^{-1}(H/(0.5W)) \quad (5)$$

$$SVF_{wall} = 0.5 (\sin^2\theta + \cos \theta - 1) (\cos \theta)^{-1} \quad (6)$$

$$SVF_{sky} = (1 - 2 SVF_{wall}) \quad (7)$$

$$SVF'_{steyn} = 0.033 + 1.004 SVF_{sky} \quad (8)$$

In addition to the above corresponding formulae, the methodology of sensitivity analysis assumes the relationship between the SVF and GnPR is mainly due to trees. The SVF value is reduced by 0.2 for every increase of 1 GnPR. The variable of the GnPR is also included in the SVF calculator. However, users should remember to only fill in the GnPR

variable when its value is determined by trees. Otherwise, the GnPR variable is 0.

Conclusion

This paper has demonstrated the development of estate-level empirical models of minimum (T_{min}), average (T_{avg}), and maximum (T_{max}) air temperature. In order to develop robust models, long-term field measurement was carried out between September 2005 and March 2008 in two green Singapore estates, NUS and One-North. The field measurement had a total of 110 measurement points, which covered various land uses.

High R^2 values of 0.86 and 0.91 have been achieved for the T_{min} and T_{avg} models, respectively. The comparison graphs of measured and calculated air temperatures have shown a good match and their differences are within the acceptable range. Meanwhile, the T_{max} model has a fair R^2 value of 0.54. It is believed that anthropogenic heat, which was not covered in the model's development, has influenced the result. However, a box and whisker plot showed that the difference between measured and calculated air temperatures is acceptable.

- Giridharan, R., Lau, S.S.Y., Ganesan, S. and Givoni, B., 2007, Urban design factors influencing heat island intensity in high rise high density environments of Hong Kong, *Building and Environment*, 42, 3669-3684.
- Giridharan, R., Lau, S.S.Y., Ganesan, S. and Givoni, B., 2008, Lowering the outdoor temperature in high-rise residential developments of coastal Hong Kong: the vegetation influence, *Building and Environment*, 43, 1583-1595.
- ISO, 1975, Standard atmosphere, ISO 2533:1975 (International Standard Organization).
- Jusuf, S.K., Wong, N.H., Hagen, E., Anggoro, R. and Yan, H., 2007, The influence of land use on the urban heat island in Singapore, *Habitat International*, 31, 232-242.
- Knowles, R.L., 1977, *Energy and form: An ecological approach to urban growth*, The MIT Press, USA.
- Kruger, E. and Givoni, B., 2007, Outdoor measurements and temperature comparisons of seven monitoring stations: preliminary studies in Curitiba, Brazil, *Building and Environment*, 42, 1685-1698.
- Laski, L. and Schellekens, S., 2007, Growing up urban. In Marshal, A. and Singer, A. (eds.), *The state of world population 2007 youth supplement*, United Nations Population Fund (UNFPA).
- Matzarakis, A., Rutz, F., and Mayer, H., 2000, Estimation and calculation of the mean radiant temperature within urban structures. In: de Dear, R.J., Kalma, J.D., Oke, T.R. and Auliciems, A.(eds.). *Biometeorology and Urban Climatology at the Turn of the Millennium. Selected Papers from the Conference ICB-ICUC'99, Sydney, WCASP-50, WMO/TD No. 1026*, 273-278.
- Oke, T.R. and Eas, C., 1971, The urban boundary layer in Montreal, *Boundary-Layer Meteorology*, 1, 411-437.
- Oke, T.R., 1981, Canyon geometry and the nocturnal urban heat island: comparison of scale model and field observations, *International Journal of Climatology*, 1(1-4), 237-254.
- Oke, T.R., Johnson, G.T., Steyn, D.G and Watson, I.D., 1991, Simulation of surface urban heat islands under 'ideal' conditions at night. Part 2: Diagnosis of causation, *Boundary-Layer Meteorology*, 56, 339-358
- Padmanabhamurty, 1990/91, Microclimates in tropical urban complexes, *Energy and Buildings*, 15 (3-4), 83-92.
- Sani, S., 1990/91, Urban climatology in Malaysia: an overview, *Energy and Buildings*, 15 (3-4), 105-117.
- Santamouris, M., 2001, The canyon effect. In: Santamouris, M. (editor). *Energy and climate in the urban built environment*, James & James Science Publishers, London.
- Swaid, H. and Hoffman M.E., 1990, Prediction of urban air temperature variations using the analytical CTTC model, *Energy and Buildings*, 14, 313-324.
- Taha, H., Akbari, H., Rosenfeld, A. and Huang, J., 1988, Residential cooling loads and the urban heat island-the effects of albedo, *Building and Environment*, 23(4), 271-283.
- Wikipedia, 2008, List of countries by population density, Retrieved on 25th September 2008 from: http://en.wikipedia.org/wiki/List_of_countries_by_population_density
- Wong, N.H. and Chen, Y., 2009, *Tropical urban heat islands: Climate, building and greenery*. Taylor and Francis, UK.
- Wong, N.H., Jusuf, S.K., La Win, A.A., Htun, K.T., Negara, T.S. and Wu, X., 2007, Environmental study of the impact of greenery in an institutional campus in the tropics, *Building and environment*, 42, 2949-2970.
- Wong, N.H. and Jusuf, S.K., Air temperature distribution and the influence of sky view factor on air temperature in a green Singapore estate, Submitted to *Journal of Urban Planning and Development*.

(Received Feb 9, 2012, Accepted Oct 10, 2012)